ENGINEERING JOURNAL

Article

Improved Synthesis of Alkali Metal Vanadates Using a Hydrothermal Method

Samroeng Krachodnok[1,a], Kenneth J. Haller[1,b,*], and Ian D. Williams[2]

1 School of Chemistry, Institute of Science, Suranaree University of Technology, Nakhon Ratchasima 30000, Thailand
2 Department of Chemistry, Hong Kong University of Science and Technology, Clear Water Bay, Kowloon, Hong Kong, People's Republic of China
3 Department of Applied Chemistry and Center for Innovation in Chemistry, Faculty of Science, Lampang Rajabhat University, Lampang 52100,
Email: krachodnok@lpru.ac.th[a], ken.haller@gmail.com[b,*]

Abstract. High product yield of highly crystalline layered $M_xV_3O_8$ compounds was obtained under hydrothermal conditions from the V_2O_5–$Zn(OAc)_2{\cdot}2H_2O$–alkali metal salt–H_2O system at significantly lower reaction temperature than previously reported in neutral media for x = 1 and M = K^+, Rb^+, and Cs^+, and in basic media for x = 2 and M = K^+. Unreacted $Zn(OAc)_2$ may act as a catalyst and/or HOAc/OAc^- acts as a buffer in obtaining monopotassium salts while enMe used to adjust pH can also act as a reducing agent in producing the dipotassium salt. A new layered dipotassium zinc pyrovanadate compound, $K_2ZnV_2O_7$, was formed when twice the stoichiometric ratio of the zinc salt was used. Single crystal X-ray diffraction shows the zinc compound to crystallize in the tetragonal space group $P4_2/mnm$ (No. 136) with a = 8.3478(16) Å, c = 11.297(3) Å, V = 787.2(3) Å^3, and thus to be isomorphous with $K_2MgV_2O_7$. The pentagonal-motif layer structure of $K_2ZnV_2O_7$ is similar to that of $K_2(VO)V_2O_7$, but the unit cell parameters differ with approximate doubling of the c axial length when replacing the square-pyramidal VO_5 units of the $[(V^{4+}O)(V^{5+}{}_2O_7)]_n^{2n-}$ layer with distorted ZnO_4 tetrahedra.

Keywords: Hydrothermal synthesis, alkali metal vanadates, pentagonal-motif layers.

ENGINEERING JOURNAL Volume 16 Issue 3
Received 22 November 2011
Accepted 28 May 2012
Published 1 July 2012
Online at http://www.engj.org/
DOI:10.4186/ej.2012.16.3.19

This paper is based on the poster presentation at the German-Thai Symposium on Nanoscience and Nanotechnology 2011—Green Nanotechnology of the Future, GTSNN 2011, in Nakhon Ratchasima, Thailand, 13-16 September 2011.

DOI:10.4186/ej.2012.16.3.19

1. Introduction

The layered main group trivanadates ($M_xV_3O_8$) are of current interest due to potential applications in Li-ion batteries [1, 2] and low-temperature magnetic devices [3]. Vanadium exhibits complex structural chemistry, associated with the different valence states (+3, +4, +5), coordination numbers, and geometries (tetrahedral, trigonal bipyramidal, square pyramidal, and octahedral) available to vanadium, that allows layers to be built up from different polyhedral connections and orientations. As a result, several different varieties of layered types have been reported [4-6].

Monopotassium trivanadate (KV_3O_8 or $K(VO)_2VO_6$) is a member of the MV_3O_8 ($M = K^+$, Rb^+, Cs^+) family [7, 8]. Dipotassium trivanadate ($K_2V_3O_8$) is a member of the mixed-valance fresnoite-type structure, ($M_2(V^{4+}O)V^{5+}{}_2O_7$; $M = K^+$, Rb^+, NH_4^+), of interest due to their low-temperature magnetic properties [3-4, 9]. This vanadate family crystallizes in the polar tetragonal space group, *P*4b*m*, and contains polymeric $[(V^{4+}O)(V^{5+}{}_2O_7)]_n^{2n-}$ layers composed of equal numbers of building units of $V^{4+}O_5$ square pyramids and $V^{5+}{}_2O_7$ pyrovanadates. The building units combine by corner-sharing basal O atoms such that all V=O groups of the plane (and of the crystal) are oriented in the same direction parallel to the *c* axis. Basal μ_2-O connections form a 2-D network of pentagonal motifs. The potassium coordination environment consists of the pentagonal μ_2-O atoms of one layer and the five associated apical V=O O atoms of the adjacent layer giving a distorted pentagonal antiprismatic KO_{10} coordination environment as shown in Fig. 1.

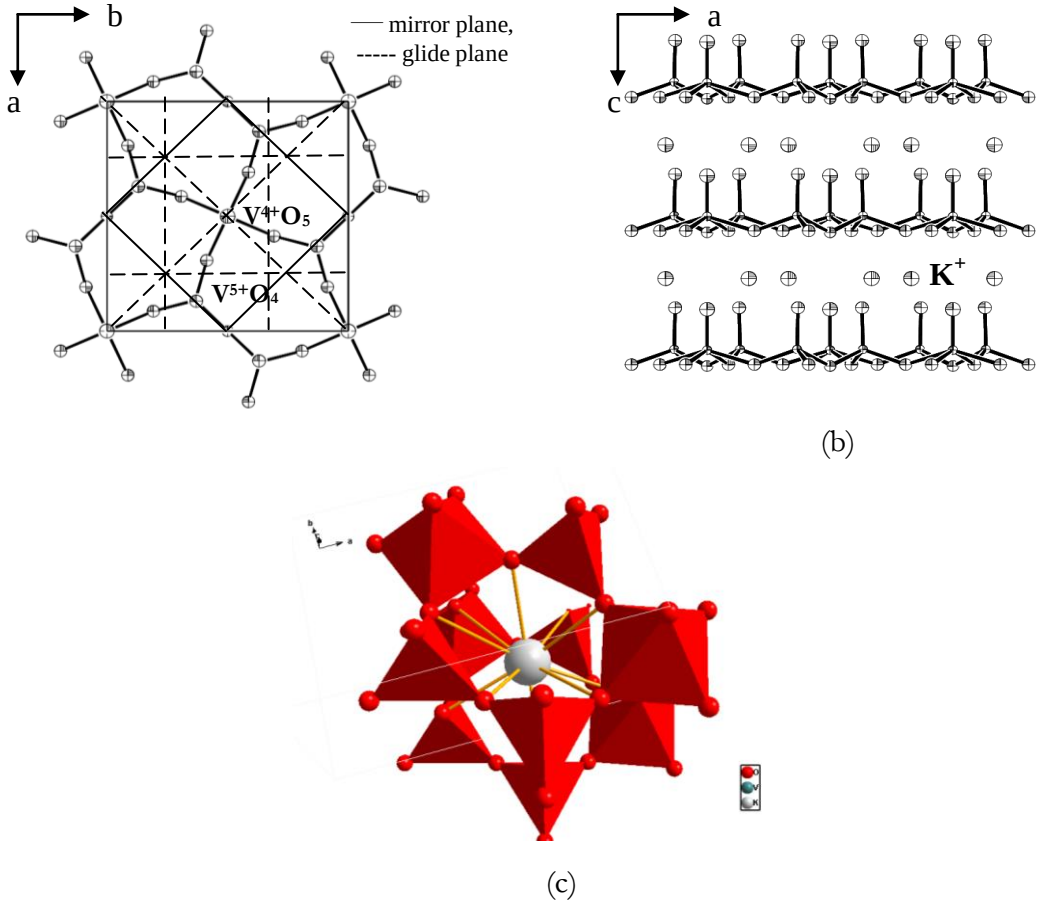

Fig. 1. Crystal structure of $K_2V_3O_8$ (a) projected onto the *ab* plane showing the $[(VO)(V_2O_7]^{2-}$ layer and (b) projected onto the *ac* plane with K^+ ions lying between layers, and (c) a perspective view of the pentagonal antiprismatic KO_{10} coordination surrounded by tetrahedral and square-pyramidal vanadium containing polyhedra [4]. (a) and (c) are in approximately the same orientation.

The melilite-type, $A_2^+B^{2+}C_2O_7$ (A = alkali metal; B = divalent metal or similar charge, and C = pyro-groups), layered vanadate structures are of interest for luminescence applications [10, 11]. They are related to the fresnoite-type structure except that the B^{2+} dication site forms distorted tetrahedra as compared to

the square pyramids of the fresnoite-type structure. The V=O groups of each V_2O_7 pyrovavadate group are oriented in opposite directions. There are two related space groups, *P*-42$_1$*m* and *P*4$_2$/*mnm*, in which all $B^{2+}C_2O_7$ layers have the same vanadium polyhedra orientations and the A^+ monocations lie between the layers in square antiprismatic coordination environment, but the two $B^{2+}C_2O_7$ layer types are related by mirror planes and two crystallographically independent A^+ form a distorted square prism, respectively. If the B^{2+} dication site is an alkaline earth metal, the compounds crystallize in the monoclinic space group *P*2$_1$/*n* with BO_6 octahedra sharing corners with pyrovanadates forming 2-D sheets of hexagonal motifs [10].

Various synthetic conditions, including reaction temperature and pH, and chemical sources affect the structure type of the products and thus, the intrinsic structure inside the crystal. Most trivanadates have been prepared at high temperature by ceramic synthesis routes [3-4,7-9,12-14] with difficulty in controlling the composition of the mixed-valence vanadium compounds as in the synthesis of $K_2(V^{4+}O)V^{5+}{}_2O_7$. Galy and Carpy [4] obtained the single crystal product from solid state reaction of the K_2O–V_2O_5–VO_2 system. Twenty years later, the same compound was produced from the solid state reaction of KVO_3, V_2O_3, and V_2O_5 in a sealed tube at 550 °C [3]. Finally, single crystals were prepared by cooling of VO_2 in molten KVO_3 flux in a platinum crucible sealed inside a silica container [9]. The mixed-cation pyrovanadate, $K_2ZnV_2O_7$, was made by heating a 1:1:1 molar mixture of K_2CO_3, ZnO, and V_2O_5 at 550 °C overnight, regrinding and heating again at 550 °C for 2 days [12].

The methods are complicated and expensive with difficulties in controlling the homogeneity, particle size, and morphology of the products. KV_3O_8 was synthesized by acidification of the corresponding metavanadate solution at near ambient temperatures of about 60-80 °C, but the quality of the single crystals was not good enough [7]. Good single crystals of KV_3O_8 were synthesized in low yield by hydrothermal reaction at 250 °C of V_2O_5 powder with alkali metal nitrate, chloride, and sulfate solution [8], later $K_2V_3O_8$ nanorods were prepared in low yield under solvothermal conditions at 200 °C employing a reducing agent and ethanol as a solvent [13], and still later tubular-windows on sheet-like $K_2V_3O_8$ single crystals were prepared in pure phase under hydrothermal conditions from KVO_3–KOH–apidic acid as a mild reducing agent, buffer, and a potentially morphological directing agent at 180 °C for 2 days [14].

This work follows up on our previous report from a similar reaction system [15] where the diamines incorporate into hybrid zinc-vanadium products. Herein we report a high yield hydrothermal synthesis of highly crystalline $M_xV_3O_8$. Reaction conditions were varied and enMe was used to adjust reaction pH and as a reducing agent. $Zn(OAc)_2$ employed as a potential catalyst in the formation of $M_xV_3O_8$ also became a Zn^{2+} source to replace VO^{2+} ions forming $K_2ZnV_2O_7$ as a product.

2. Experimental

2.1. Chemicals and Instrumentation

All reagents were used as received. All syntheses were carried out in PTFE-lined stainless steel reactors under autogenous pressure. The 23 mL reaction vessels were filled to approximately 40% volume capacity. Powder X-ray diffraction patterns were recorded on a Philips PW1830 diffractometer equipped with a Cu *Ka* X-ray source ($\overline{\lambda}$ = 1.54062 Å) in the angular range 2θ = 5-50°, with 0.05° step size and 3 s per step counting time. XRD pattern analyses were carried out by the Traces program version 3. Single crystal X-ray diffraction characterization utilized a Bruker Smart Apex CCD diffractometer equipped with a graphite-monochromated Mo *Ka* X-radiation source ($\overline{\lambda}$ = 0.71073 Å) and standard Bruker software [16]. Infrared spectra of the samples were recorded using pressed KBr pellets on a Perkin-Elmer Spectrum GX FTIR spectrophotometer in the range of 650-1100 cm^{-1} (5 scans, resolution 4 cm^{-1}).

2.2. Synthesis of Monopotassium (or Rubidium or Cesium) Trivanadates, MV_3O_8

V_2O_5 (181 mg), $Zn(OAc)_2{\cdot}2H_2O$ (220 mg), KOH (56 mg) or RbCl (121 mg) or CsCl (168 mg), and water (2.0 mL), mole ratio 1:1:1:111 were heated at 110, 160, and 200 °C for 2 days. Initial and final reaction pH was ~7 without adjustment. Orange plates of AV_3O_8 were isolated with product yields as in Table 1. Selected FT-IR bands (cm^{-1}): KV_3O_8, 990 (w), 959 (s) and 737 (br); RbV_3O_8, 1005 (m), 967 (s, sh) and 780 (sh), and 737 (br); and CsV_3O_8, 1000 (m), 963 (s), 783 (sh), and 741 (br).

Table 1. Product Yields of $M_xV_3O_8$ (Based on V_2O_5) as a Function of Temperature.

Compound	Reaction Temperature		
	110 °C	160 °C	200 °C
KV_3O_8	66 %	87 %	90 %
RbV_3O_8	86 %	88 %	90 %
CsV_3O_8	91 %	94 %	100 %
$K_2V_3O_8$	60 %	80 % [a]	40 % [b]
$K_2ZnV_2O_7$	5 %		

[a] *Reaction temperature for $K_2V_3O_8$ of 140 °C.*

[b] *The yield of $K_2V_3O_8$ for reaction temperature of 180 °C was 50 %.*

2.3. Synthesis of Dipotassium Trivanadate, $K_2V_3O_8$

V_2O_5 (181 mg), $Zn(OAc)_2{\cdot}2H_2O$ (220 mg), KOH (56 mg), and water (2.0 mL), mole ratio 1:1:1:111 were heated at 110 °C for 2 days. Initial reaction pH was adjusted to ~11 with enMe. Final reaction pH was ~9. Black plates of $K_2V_3O_8$ (yield ~60%, based on V_2O_5) were obtained as the major product with a small amount of black powder, $(HenMe)_2ZnV_8O_{20}$ [15], as a minor product. The highest product yield (~80 %, based on V_2O_5) was obtained by increasing reaction temperature to 140 °C. The yield decreased with increasing reaction temperature above 140 °C (yield ~40 % at 200 °C). Selected FT-IR bands (cm^{-1}): 991 (m), 940 (w), 926 (vw), 817 (br) and 740 (br).

2.4. Synthesis of Dipotassium Zinc Pyrovanadate, $K_2ZnV_2O_7$

Procedure similar to that for $K_2V_3O_8$ except twice the stoichiometric amount of $Zn(OAc)_2{\cdot}2H_2O$ (2.0 mmol) was used. Heating at 110 °C for 2 days gave a mixture of black plates of $K_2V_3O_8$, black blocks of $Zn(HenMe)_2V_8O_{20}$, and colorless needles of $K_2ZnV_2O_7$ with yields of ~60 %, ~35%, and ~5%, respectively, based on V_2O_5. Selected FT-IR bands (cm^{-1}): 936 (br), 896 (br), 851 (br) and 691 (br).

2.5. X-ray Crystallography

A single crystal of $K_2ZnV_2O_7$ suitable for single-crystal X-ray diffraction with size 0.01 x 0.01 x 0.30 mm was used. Unit cell parameters and space group were determined by standard procedures [16] from data collected on a Bruker Smart Apex CCD diffractometer at 100±2 K. Crystal data are given in Table 2. The new compound is isomorphous with $K_2MgV_2O_7$ [17].

Table 2. Crystal Data for $K_2ZnV_2O_7$.

Crystal Data for $K_2ZnV_2O_7$	
Chemical formula	$K_2O_7V_2Zn$
M_r (Daltons)	178.72
Temperature (K)	100±2
Crystal system, space group	Tetragonal, $P4_2/mnm$
Unit cell parameters: a, (Å)	8.3478(16)
c, (Å)	11.297(3)
V, (Å^3)	787.2(3)
Z	2
D_{calc} (Mg m^{-3})	1.508

3. Results and Discussion

3.1. Hydrothermal Synthesis

Four $M_xV_3O_8$ compounds were synthesized using water as an environmentally friendly solvent in the hydrothermal reaction of V_2O_5 and $Zn(OAc)_2{\cdot}2H_2O$ with alkali metal sources (KOH, RbCl, CsCl) in the mole ratio of 1:1:1 in 2-day reactions. Previous work had found that both reaction pH and temperature play crucial roles in determining the isolated solid product [18], and that the nature of organic sources and solvent could lead to reduction of oxidation state of the transition metal and/or control of size and morphology of the crystal products [13, 14]. With x = 1 and M = K^+, Rb^+, Cs^+, orange plates were formed in neutral media at 110 °C without an organic source, whereas for x = 2 and M = K^+, phase-pure black plates, similar to those of [14], were isolated from basic media at 140 °C, using an organic base (enMe) to adjust pH and act as a reducing agent. Acetic acid/acetate in this work may be similar to apidic acid/apidate in [14] which is suggested to act as a buffer. The acidic aqueous solvent gives plate morphology, compared to the nanorods obtained under solvothermal reaction conditions employing ethanol as solvent and reducing agent [13]. While the organic reactants and solvent are crucial factors, vanadium oxide sources seem to have no effect on the size and morphology of the product (including acidity with V_2O_5 observed herein and previously [13] and basicity with KVO_3 [14]). Zinc acetate acts as a good catalyst in the formation of $K_2V_3O_8$ with relatively higher yield than previously obtained, but with the yield limited due to Zn^{2+} competing with VO^{2+} ions forming $K_2ZnV_2O_7$ with increasing amounts of $Zn(OAc)_2{\cdot}2H_2O$.

3.2. XRD patterns

Experimental XRD patterns of bulk samples of all compounds are compared to the simulated XRD patterns calculated from previously reported single crystal X-ray structural results [8] in Fig. 2. The patterns indicate highly crystalline pure phase products at all reaction temperatures with increasing crystallinity, as shown by increasing intensity and sharpening of the XRD peaks [2], as reaction temperature increases.

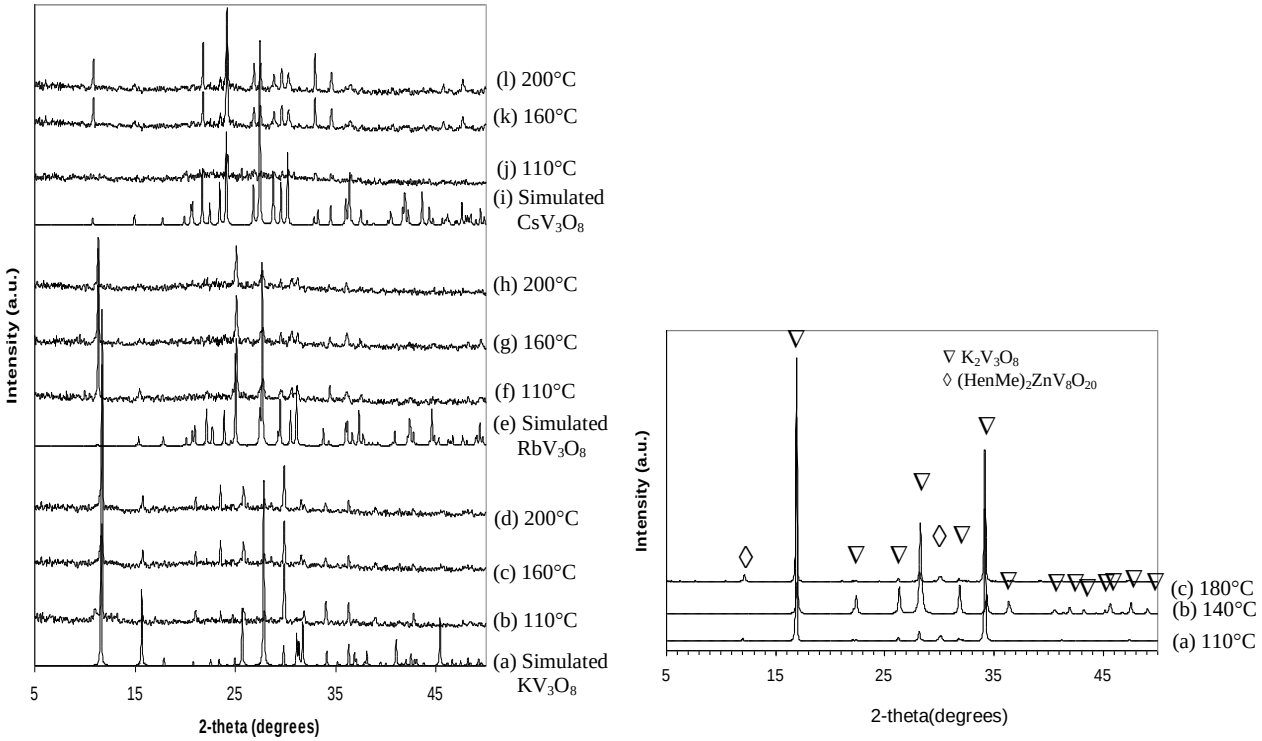

(a) MV_3O_8 (b) $K_2V_3O_8$

Fig. 2. Simulated and experimental XRD patterns for MV_3O_8 and $K_2V_3O_8$.

The XRD patterns of MV_3O_8 (Fig. 2(a)) also show highest crystallity for the MV_3O_8 phase at 200 °C. Fewer diffraction peaks are observed for RbV_3O_8 and CsV_3O_8 relative to KV_3O_8, indicating lower crystallity in spite of the higher yields of 86 % and 91 %, respectively, even at 110 °C. Unreacted zinc acetate may possibly act as a catalyst [19], significantly reducing reaction temperature to near 100 °C for obtaining MV_3O_8 compounds as reported herein compared to 250 °C reported previously [8].

The XRD patterns of $K_2V_3O_8$ (Fig. 2(b)) also show highly crystalline phase $K_2V_3O_8$ at the optimum reaction temperature of 140 °C (~80 % yield), significantly lower by 40 °C compared to the previous hydrothermal reaction in slightly acidic (pH 4.5-6) solution [14] and by 60 °C compared to the solvothermal reaction [13]. Unreacted zinc acetate is presumed to act as a catalyst [19] as noted above. At lower or higher reaction temperatures than at 140 °C, black crystals of the 3-D nanoporous material $(HenMe)_2ZnV_8O_{20}$ [15], were also formed.

3.3. The Crystal Structure of $K_2ZnV_2O_7$

Single crystal X-ray diffraction shows $K_2ZnV_2O_7$ to be isomorphous to $K_2MgV_2O_7$ [17] with tetragonal space group $P4_2/mnm$ (No. 136). The c axis length is double that of $K_2V_3O_8$, space group $P4bm$, consistent with the existence of the mirror plane perpendicular to the [001] direction between two $[BV_2O_7]_n^{2n-}$ layers (B = Mg in [17] and Zn herein). The structure contains $[ZnV_2O_7]_n^{2n-}$ layers with K^+ positioned between the layers forming two unique distorted square-prismatic KO_8 coordination environments as can be seen in Fig. 3.

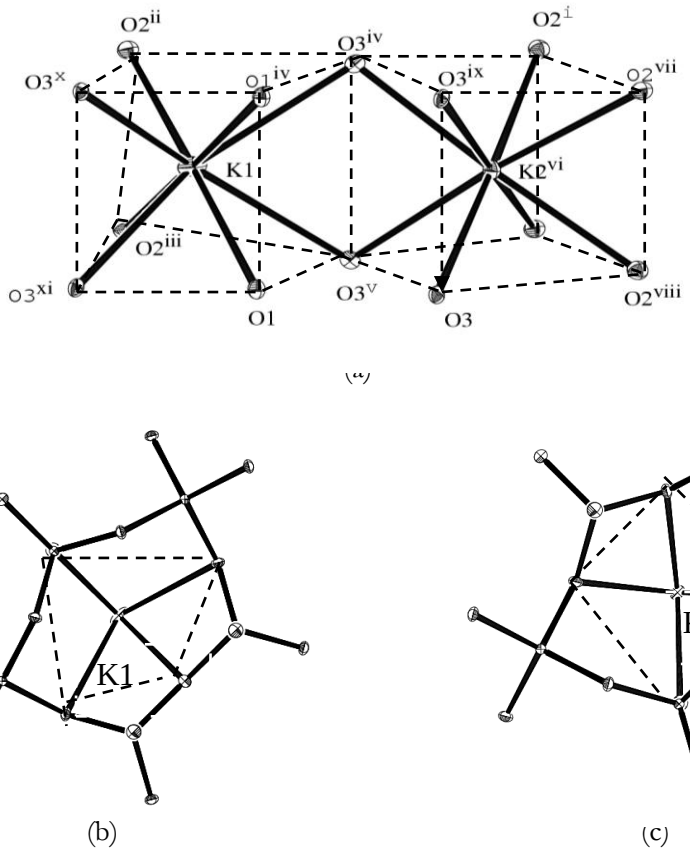

Fig. 3. (a) Perspective view of the distorted square prismatic environments of the K^+ ions and projection views of (b) K(1) and (c) K(2) in the centers of the pentagonal channels in $K_2ZnV_2O_7$.

The layer consists of equal numbers of the two building units; the tetrahedral ZnO_4 units lying on -4 sites at $0,{}^1/_2,z$ and ${}^1/_2,0,z$ ($z = {}^1/_4$ and ${}^3/_4$) and V_2O_7 units positioned on *2.mm* sites similar to those observed in $K_2V_3O_8$ (Fig. 4(d)) except the V=O groups of pyrovanadate units are oriented in opposite directions while they are oriented in the same direction in $K_2V_3O_8$. The interlayer spacing is 3.230 Å and similar to that observed in $K_2MgV_2O_7$ [17], but larger than the 3.055 Å in $K_2(VO)V_2O_7$ [20] and smaller than the 3.477 Å in $Rb_2MnV_2O_7$ and the 3.444 Å in $KRbMnV_2O_7$ [21]. The O–Zn–O angles of 114.25(13)°

show smaller deviation from normal tetrahedral geometry compared to the O–Mn–O angles, 121.05(7), 117.4(2)°, 115.63(19)°, and 115(1)°, in $K_2MnV_2O_7$, $Rb_2MnV_2O_7$, $KRbMnV_2O_7$, and $K_2MnV_2O_7$, respectively. The V–O bond distances and the O–V–O angles are in the normal range, similar to those observed in $Rb_2MnV_2O_7$ and $KRbMnV_2O_7$.

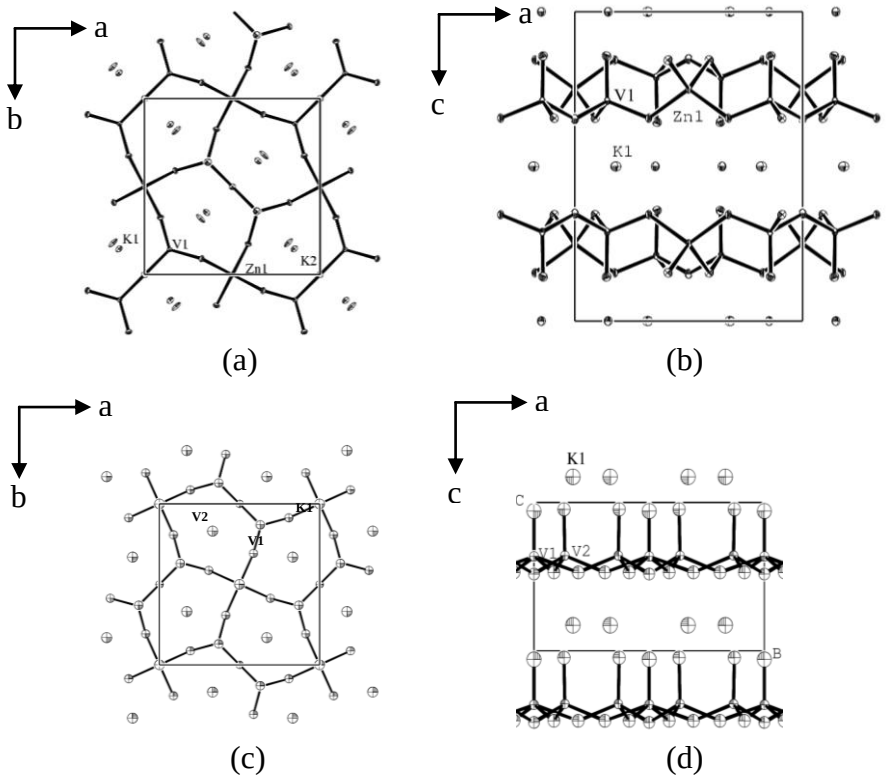

Fig. 4. Comparing the $[ZnV_2O_7]^{2-}$ layer (a) projected onto the *ab* plane and (b) on the *ac* plane, with the $[(V^{4+}O)V_2O_7]^{2-}$ layer (c) projected onto the *ab* plane and (d) on the *ac* plane; after [20].

3.4 Infrared Spectroscopy

Figure 5 shows FT-IR spectra of the vanadates. The spectrum of CsV_3O_8 has medium and strong absorption peaks at 1000 and 963 cm^{-1} due to the vibration modes of two distinct V=O units. While the shorter V=O bond, at axial position of $V^{5+}O_6$ octahedra has d[V=O(1)] = 1.599(9) Å and the longer bonds at apical positions of $V^{5+}O_5$ square pyramids have d[V=O(4)] = 1.602(7) Å, this slight difference in distance, 0.003 Å, is not statistically significant. The significantly different distances involve V=O O atoms connecting to the MO_8 coordination motif where d[K–O(1)] = 3.093(9) Å, with a shorter distance of 0.006 and 0.105 Å compared to other d[K–O(4)] = 3.098(6) and 3.197(6) Å, respectively. Comparing these IR peaks with those of isostructural compounds; 1005 and 967 cm^{-1} for Rb, and 990 and 959 cm^{-1} for K, suggest the V=O bond distance of CsV_3O_8 is shorter than in KV_3O_8 and longer than RbV_3O_8, not in agreement with those observed by Oka *et al.* [8]. The broad absorption peak near 740 cm^{-1}, and the shoulders near 780 cm^{-1} are assigned to the antisymmetric stretching and bending modes of the $V–O_b$ bond and V–O–V bridges, however, it is very difficult to correlate and classify the O_b bond, where b are bridging O atoms, with bending modes from infrared spectroscopy.

For $K_2V_3O_8$, the strong and very weak absorption peaks at 991 and 940 cm^{-1} are assigned to the vibrational modes of two V=O bonds at apical positions of $V^{4+}O_5$ square pyramid and $V^{5+}O_4$ tetrahedra along the *c* axis, d[V=O_t] = 1.582(6) and 1.628(11) Å, respectively, due to the five associated apical V=O O atoms of pentagonal antiprismatic KO_{10} coordination environment. There are three shorter bonds, d[K–O] = 2.769(11) and 2.904(11) Å and one longer bond, d[K–O] = 3.512(6) Å, related to apical positions of square pyramids and tetrahedra, respectively. Three absorption peaks at 926, 817, and 740 cm^{-1} are assigned to the antisymmetric stretching and bending modes of bridging $V–O_b–V$ units related to the 2-D vanadium and basal-plane oxygen atoms in the *ab* plane [4, 9, 14, 20].

The broad bands at 936, 896 and 851 cm^{-1} in the IR spectrum of $K_2ZnV_2O_7$ correspond to the vanadate bonds with distances of 1.643(3), 1.707(2) and 1.806(2) Å [22], and the broad peak at 691 cm^{-1} is assigned to the bending mode of the bridging V–O_b–V units.

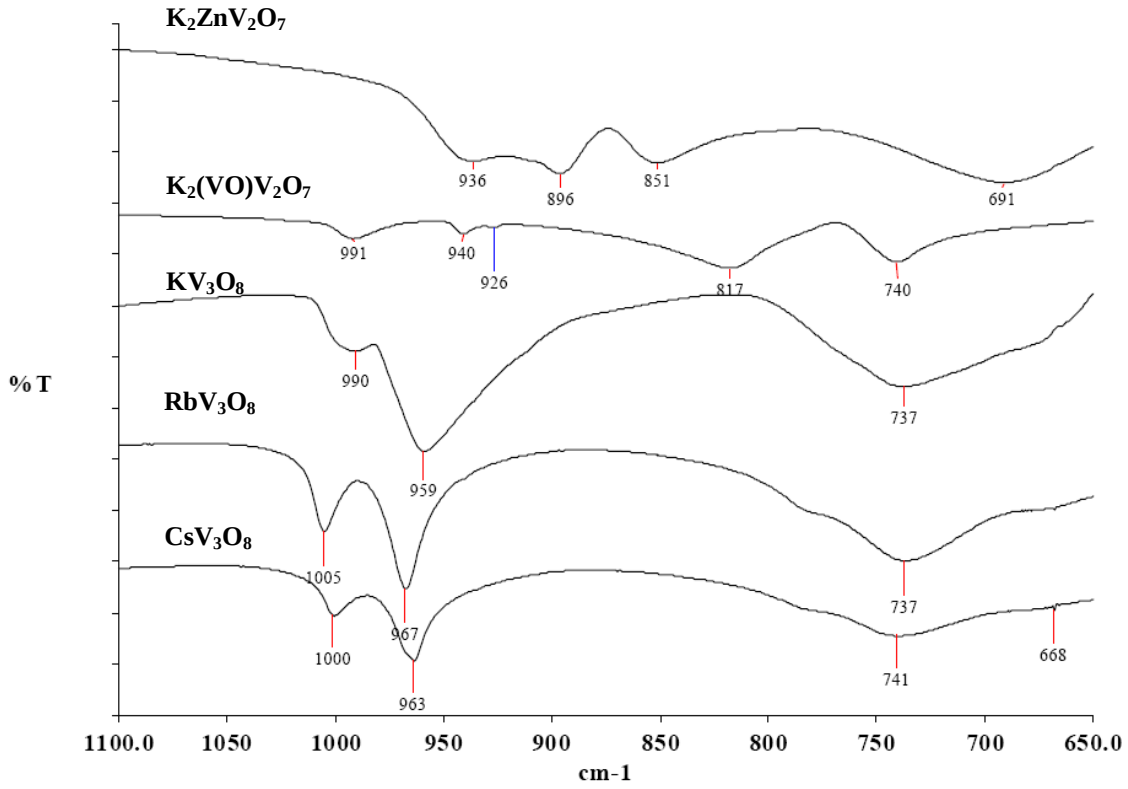

Fig. 5. FT-IR spectra of alkali metal vanadates.

4. Conclusions

Four layered trivanadate compounds have been prepared in high yield by hydrothermal synthesis from V_2O_5 and KOH in mole ratio 1:1 (MV_3O_8, M = K, Rb, and Cs, in neutral media, and mixed valence $K_2V_3O_8$ in basic media) with reaction temperature lower than previous reports due to zinc acetate possibly acting as catalyst and enMe, in the latter case, as a reductant to reduce V^{5+} to V^{4+} as well as in ethanol. The new mixed cation pyrovanadate, $K_2ZnV_2O_7$, formed as a competing product when the quantity of zinc acetate catalyst was increased. This simple, inexpensive, and environmentally friendly hydrothermal preparation route can be developed to prepare other layered vanadates systems.

References

[1] G. Li, S. Pang, L. Jiang, Z. Guo, and Z. Zhang, "Environmentally friendly chemical route to vanadium oxide single-crystalline nanobelts as a cathode material for lithium-ion batteries," *J. Phys. Chem. B,* vol. 110, no. 19, pp. 9383-9386, 2006.

[2] H. Yang, J. Li, X.-G. Zhang, and Y.-L. Jin, "Synthesis of LiV_3O_8 nanocrystallites as cathode materials for lithium ion batteries," *J.* Mat. *Process. Tech.*, vol. 207, no. 1-3, pp. 265-270, 2008.

[3] G. Liu and J. E. Greedan, "Magnetic properties of fresnoite-type vanadium oxides: $A_2V_3O_8$ (A = K, Rb, NH_4)," *J. Solid State Chem.,* vol. 114, no. 1, pp. 499-505, 1995.

[4] J. Galy and A. Carpy, "Structure crystalline de $K_2V_3O_8$ ou $K_2(VO)[V_2O_7]$," *Acta Cryst. Sect. B*, vol. 31, no. 6, pp. 1794-1795, 1975.

[5] D. Riou and G. Férey, "Intercalated vanadyl vanadates: syntheses, crystal structures, and magnetic properties," *Inorg. Chem*, vol. 34, no. 26, pp. 6520-6523, 1995.

[6] Y. Zhang, R. C. Haushalter, and A. Clearfield, "Hydrothermal syntheses and structural characterization of layered vanadium oxides incorporating organic cations: *a-,β-*

$(H_3N(CH_2)_2NH_3)[V_4O_{10}]$ and *a*-,*β*-$(H_2N(C_2H_4)_2NH_2)[V_4O_{10}]$," *Inorg. Chem.*, vol. 35, no. 17, pp. 4950-4956, 1996.

[7] H. T. Evans and S. Block, "The crystal structures of potassium and cesium trivanadates," *Inorg. Chem.*, vol. 5, no. 10, pp. 1808-1814, 1966.

[8] Y. Oka, T. Yao, and N. Yamamoto, "Hydrothermal synthesis and structure refinements of alkali-metal trivanadates MV_3O_8 (M = K, Rb, Cs)," *Mat. Res. Bull.*, vol. 32, no. 9, pp. 1201-1209, 1997.

[9] L. Choi, Z. T. Zhu, J. L. Musfeldt, G. Ragghianti, D. Mandrus, B. C. Sales, and J. R. Thompson, "Local symmetry breaking in $K_2V_3O_8$ as studied by infrared spectroscopy," *Phys. Rev. B*, vol. 65, no. 5, pp. 54101-54106, 2001.

[10] V. G. Zubkov, A. P. Tyutyunnik, N. V. Tarakina, I. F. Berger, L. L. Surat, B. V. Slobodin, G. Svensson, B. Forslund, B. V. Shulgin, V. A. Pustovarov, A. V. Ishchenko, and A. N. Cherepanov, "Synthesis, crystal structure and luminescent properties of pyrovanadates $M_2CaV_2O_7$ (M = Rb, Cs)," *Solid State Sci.*, vol. 11, no. 3, pp. 726-732, 2009.

[11] B. V. Slobodin, L. L. Surat, R. F. Samigullina, A. V. Ishchenko, B. V.,Shulgin, and A. N. Cherepanov, "Thermochemical and luminescent properties of the $K_2MgV_2O_7$ and $M_2CaV_2O_7$ (M = K, Rb, Cs) vanadates," *Inorg. Mat.*, vol. 46, no. 5, pp. 522-528, 2010.

[12] H. McMurdie, M. Morris, E. Evans, B. Paretzkin, W. Wong-Ng, and Y. Zhang, "Standard x-ray diffraction powder patterns from the JCPDS Research Associateship," *Powder Diffraction*, vol. 1, no. 4, p. 343, 1986.

[13] H. Xu, W. He, H. Wang, and H. Yan, "Solvothermal synthesis of $K_2V_3O_8$ nanorods," *J. Cryst. Growth*, vol. 260, no. 3, pp. 447-450, 2004.

[14] F.-N. Shi, J. Rocha, A. B. Lopes, and T. Trindade, "Morphological micro-patterning of tubular-windows on crystalline $K_2V_3O_8$ sheets," *J. Cryst. Growth*, vol. 273, no. 3-4, pp. 572-576, 2005.

[15] S. Krachodnok, K. J. Haller, and I. D. Williams, "Hydrothermal synthesis of three-dimensional nanoporous zinc vanadates: $(HenMe)_2ZnV^{4+}{}_4V^{5+}{}_4O_{20}$ and $(enMe)_2Zn(VO_3)_2{\cdot}2H_2O$ containing pillared/layered structure," in *Proceedings of the German-Thai Symposium on Nanoscience and Nanotechnology*, Bangkok, 2007, pp. 63-68.

[16] Bruker, SMART (Version 5.625) and SAINT (Version 6.26a), Bruker Analytical X-ray Systems Inc., Madison, Wisconsin, USA, 2001.

[17] E. V. Murashova, V. K. Velikodnyi, and V. K. Trunov, "Structure of the double pyrovanadate $K_2MgV_2O_7$," *Z. Neorganicheskoi Khimii*, vol. 33, no. 6, pp. 1593-1595, 1988.

[18] T. S.-C. Law and I. D. Williams, "Organic-directed synthesis of manganese vanadates with variable stoichiometry and dimensionality: 1-D $[(Hen)_2Mn(VO_3)_4]$, 2-D $[(H_2en)_2[Mn(VO_3)_4]$, and 3-D $[(H_2en)[MnF(VO_3)_3]$," *Chem. Materials*, vol. 12, no. 1, pp. 2070-2072, 2000.

[19] X. Zhao, Y. Zhang, and Y. Wang, "Synthesis of propylene carbonate from urea and 1,2-propylene glycol over a zinc acetate catalyst," *Ind. & Eng. Chem. Res.*, vol. 43, no. 15, pp. 4038-4042, 2004.

[20] B. C. Chakoumakos, R. Custelcean, T. Kamiyama, K. Oikawa, B. C. Sales, and M. D. Lumsden, "Structural modulation in $K_2V_3O_8$," *J. Solid State Chem.*, vol. 180, no. 3, pp. 812-817, 2007.

[21] H. B. Yahia, E. Guadin, and J. Darriet, "Crystal structures of new pyrovanadates $A_2MnV_2O_7$ (A = Rb, K)," *Z. Naturforschung B*, vol. 62, no. 7, pp. 873-880, 2007.

[22] S. Krachodnok, "Syntheses and Structural Studies of Organically Modified Main Group Vanadates," Ph.D. thesis, Suranaree University of Technology, 2010.